

1 A bivariate extension of the Hosking and Wallis
2 goodness-of-fit measure for regional distributions

T. R. Kjeldsen,¹ and I. Prosdocimi²

Corresponding author: T. R. Kjeldsen, Department of Architecture and Civil Engineering, University of Bath, Claverton Downs, Bath, BA2 7AY, United Kingdom. (t.r.kjeldsen@bath.ac.uk)

¹Department of Architecture and Civil Engineering, University of Bath, Claverton Downs, Bath, BA2 7AY, United Kingdom.

²Centre for Ecology & Hydrology, Maclean Building, Wallingford, OX10 8BB, United Kingdom.

3 **Abstract.** This study presents a bivariate extension of the goodness-of-
4 fit measure for regional frequency distributions developed by *Hosking and*
5 *Wallis* [1993] for use with the method of L-moments. Utilising the approx-
6 imate joint normal distribution of the regional L-skewness and L-kurtosis,
7 a graphical representation of the confidence region on the L-moment diagram
8 can be constructed as an ellipsoid. Candidate distributions can then be ac-
9 cepted where the corresponding theoretical relationship between the L-skewness
10 and L-kurtosis intersects the confidence region, and the chosen distribution
11 would be the one that minimises the Mahalanobis distance measure. Based
12 on a set of Monte Carlo simulations it is demonstrated that the new bivari-
13 ate measure generally selects the true population distribution more frequently
14 than the original method. Results are presented to show that the new mea-
15 sure remains robust when applied to regions where the level of inter-site cor-
16 relation is at a level found in real world regions. Finally the method is ap-
17 plied to two different case studies involving annual maximum peak flow data
18 from Italian and British catchments to identify suitable regional frequency
19 distributions.

1. Introduction

20 The seminal work of *Hosking* [1990], *Hosking and Wallis* [1993, 1997] and others [e.g. *Vogel and Fennessey*, 1993; *Institute of Hydrology*, 1999] popularised the use of L-moments
21 and L-moment ratios in regional frequency analysis of environmental extremes such as
22 floods. In particular, *Hosking and Wallis* [1997] presented a seemingly complete and
23 robust framework for using the index flood method in combination with the method of
24 L-moment, including measures for identifying discordant data series, assessing the homo-
25 geneity of regions, and evaluation of the goodness-of-fit of regional statistical distributions.
26 This framework has been used by numerous researchers to develop regional flood frequency
27 tools for many different geographical regions, e.g. *Vogel et al.* [1993], *Mkhandi et al.* [2000],
28 and *Kumar et al.* [2003].
29

30 The results from simulation experiments reported by *Hosking and Wallis* [1997] showed
31 that regional frequency analysis is generally more accurate than at-site analysis, especially
32 for design events with very high return periods in excess of 1000 years. At the same
33 time *Hosking and Wallis* [1997] reported that misspecification of the underlying regional
34 frequency distribution becomes an important factor when considering design events with
35 return periods in excess of 100 years. Thus, correctly specifying the regional distribution
36 is a key task in order to fully capitalise on the benefits of regional frequency analysis.

37 Different methods for elucidating regional frequency distributions have been developed
38 based on L-moment diagrams. Examples include the goodness-of-fit (GOF) measure pre-
39 sented by *Hosking and Wallis* [1993] in the form of a test statistic of a normal variate
40 where the significance of the difference between a sample value of the regional L-kurtosis

41 and a set of theoretical values corresponding to different 3-parameter distributions is as-
42 sessed using Monte Carlo simulations. *Vogel et al.* [1993] recommended using the location
43 of the regional mean of the L-moment ratio on the L-moment ratio diagram as a guide for
44 the choice of an appropriate model. *Peel et al.* [2001] compared two different graphical
45 methods for assessing the regional distribution based on L-moment diagrams, a sample av-
46 erage and a line of best fit through the sample L-moment ratios. They concluded that the
47 sample mean was the most reliable method. *Madsen et al.* [1997] found that use of partial
48 duration series data led to a less ambiguous interpretation of the L-moment diagram than
49 the application of annual maximum series. Other researchers [e.g. *Liou et al.*, 2008; *Wu*
50 *et al.*, 2012; *Wang and Hutson*, 2013] have utilised the approximate normal distribution
51 of the L-moment ratios to develop graphical representations on a L-moment diagram of
52 the confidence regions obtained from a single site. Based on the work of these researchers,
53 the objective of this paper is to develop a graphical bivariate extension of the Hosking
54 and Wallis (HW) GOF measure for selecting regional distributions. Where the original
55 Hosking and Wallis GOF measure considered only the variability of the L-kurtosis, the
56 new bivariate version introduced in this paper will consider variability in both L-skewness
57 and L-kurtosis, as well as the correlation between the two. In addition, the new measure
58 has a more direct visual interpretation on the L-moment diagram. First, the assumptions
59 underpinning the index flood method will be discussed and used for developing the new
60 bivariate GOF measure. Next, a series of Monte Carlo experiments will be conducted to
61 assess the ability of the new measure to detect the correct distribution, especially when
62 compared to the original HW measure. Finally, the new measure will be applied to two
63 case studies; a homogeneous region of peak flow series from Italy, and a national study

64 using pooling groups formed using annual maximum (AMAX) series of peak flow from
 65 gauging stations located in the United Kingdom.

2. A general framework for the index flood method

2.1. The statistical model of a homogeneous region

The starting point for the statistical model underpinning the index flood method is to assume that N sites form a homogeneous region, and that at each site n_i years of independent annual maximum (AMAX) data are available, from which the sample L-moment ratios can be derived. The definition of L-moments is well documented by *Hosking and Wallis* [1997] and others and therefore not repeated here. The observed r -th order L-moment ratio at the i -th site, $t_r^{(i)}$, is defined as the true, but unknown, value for the homogeneous region, τ_r , plus an error, ε_i , because the sample value is derived from a finite number (n_i) of observations, i.e.

$$t_r^{(i)} = \tau_r + \varepsilon_i, \quad r = 2, 3, 4, \quad i = 1, \dots, N \quad (1)$$

This study will consider only $r = 2, 3, 4$ denoted L CV, L-skewness and L-kurtosis. The variance-covariances of the sample L-moment ratios are assumed inversely proportional to the sample size (record-length) [*Hosking*, 1986], and are given as a set of the covariance matrices Σ_{rq} with elements (i, j) defined as

$$\Sigma_{rq,ij} = \text{cov} \left(t_r^{(i)}, t_q^{(j)} \right) \quad (2)$$

66 where diagonal elements ($i = j$) represent the variance of the r -th L-moment ratio at
 67 each of the N sites, and the non-diagonal elements represent the covariance between the
 68 r -th and q -th L-moment ratios at different sites ($i \neq j$). Estimating the elements of these
 69 covariance matrices will be discussed later.

The regional estimate of the r -th order L-moment ratio is derived as a weighted average

$$t_r^R = \sum_{i=1}^N \omega_r^{(i)} t_r^{(i)} = \omega_r^T \mathbf{t}_r \quad (3)$$

where \mathbf{t}_r is a vector containing the r -th order L-moment ratio for each of the N sites, and ω_r is a $n \times 1$ vector of weights assigned to each individual site in the region and which sum to one, i.e. $\sum \omega_r^{(i)} = 1$. The variance of the regional L-moment ratio of the r -th order (Eq. 3) is a scalar but can be expressed as a matrix multiplication as

$$\sigma_r^2 = \text{var}(t_r^R) = \text{var}(\omega_r^T \mathbf{t}_r) = \omega_r^T \Sigma_{rr} \omega_r \quad (4)$$

where the covariance matrix Σ_{rr} is defined in Eq. (2). Similarly, the covariance between the regional L-moment ratios can be derived as

$$\sigma_{rq} = \text{cov}(t_r^R, t_q^R) = \text{cov}(\omega_r^T \mathbf{t}_r, \omega_q^T \mathbf{t}_q) = \omega_r^T \Sigma_{rq} \omega_q^T \quad (5)$$

Using the method of Lagrange multipliers for constraint optimisation the set of weights which gives the minimal variance of the regional L-moment ratio can be derived from Eq.(4) as

$$\omega_r = \Sigma_{rr}^{-1} \mathbf{i} (\mathbf{i}^T \Sigma_{rr}^{-1} \mathbf{i})^{-1} \quad (6)$$

70 where \mathbf{i} is a vector where all elements equal one. In the simplest case where no correlation
 71 exists between AMAX records across sites, and the samples are drawn from a homogeneous
 72 region, then the weights reduce to the record-length weighting procedure suggested by
 73 *Hosking and Wallis* [1997], and also used in this study. Next, the joint distribution of the
 74 L-skewness and the L-kurtosis is discussed, which will subsequently be used to developed
 75 a graphical version of the GOF measure presented by *Hosking and Wallis* [1993].

2.2. Bivariate distribution of L-skewness and L-kurtosis

In line with other researchers, notably *Hosking and Wallis* [1997] and *Liou et al.* [2008], it is assumed that the joint distribution of L-skewness and L-kurtosis is a bivariate normal distribution. As the regional L-moment ratios (t_3^R, t_4^R) are weighted averages of the at-site L-moment ratios, it follows by virtue of the central limit theorem that (t_3^R, t_4^R) is approximately distributed according to a bivariate normal distribution with a covariance matrix $\mathbf{\Omega}$ whose elements are defined by the expressions in Eqs.(4) and (5).

$$\mathbf{\Omega} = \begin{bmatrix} \sigma_3^2 & \sigma_{34} \\ \sigma_{34} & \sigma_4^2 \end{bmatrix} \quad (7)$$

For selected one and two parameter distributions, *Hosking* [1986] provided analytical expressions for the variance and covariance of L-skewness and L-kurtosis, i.e. the elements of $\mathbf{\Sigma}_{\mathbf{r}\mathbf{q}}$ in Eq.(2), and thus by extension $\mathbf{\Omega}$ in Eq.(7) . However, for distributions of more than two parameters, the analytical expressions quickly become intractable; if they exist at all. Alternative analytical expressions can be derived using approximations, but they have generally been found to be inaccurate for sample sizes typically used in hydrology. Thus, a purely analytical approach to the specification of $\mathbf{\Omega}$ appears to have limited practical utility and will not be pursued further here. Other researchers have used extensive Monte Carlo simulations to derive approximations of the sampling variability of L-moment ratios [*Sankarasubramanian and Srinivasan*, 1999], but these are only available for a specific subset of distributions. The *Hosking and Wallis* [1993] goodness-of-fit measure, hereafter referred to as the HW measure, was developed specifically to enable assessment of the goodness-of-fit of several candidate three parameter distributions, and resorted to the use of Monte Carlo simulations from a 4-parameter Kappa distribution to obtain the variance of the regional L-moment ratios. This method has the advantage that it makes no explicit prior assumption on the type of distribution being assessed. *Wang and Hutson*

[2013] suggest that a well-defined GOF test based on a distribution-specific null-hypothesis might be more powerful than a more general model selection procedure such as the HW measure. However, the widespread use of the HW measure in the analysis of environmental extreme data is a testament to the usefulness of such a procedure for screening of noisy environmental data before committing to a particular distribution model; a point also emphasised by *Wang and Hutson* [2013].

3. Goodness of fit measures for regional distributions

3.1. The Hosking and Wallis Goodness-of-fit measure

Assuming a homogeneous region, the scatter of points on the L-moment diagram around the regional average values represents only sampling variability as per Eq. (1). The HW measure reduces the two-dimensional scatter (in both L-skewness and L-kurtosis directions) to a one dimension problem by assessing the bias corrected difference between the regional average L-kurtosis, i.e. t_4^R , with the notionally true value of L-kurtosis, τ_4^{DIST} , which can be calculated as a function of L-skewness for a range of distributions using the polynomial approximations provided by *Hosking and Wallis* [1997] in their Table A.3. A schematic representation of the measure, adopted from *Hosking and Wallis* [1993], is shown in Figure 1 in the left panel. Utilising that the L-moment ratios are approximately normally distributed, the HW measure takes the form of a univariate significance test

$$Z^{DIST} = \frac{\tau_4^{DIST} - t_4^R + B_4}{\sigma_4} \quad (8)$$

where B_4 is the bias correction of t_4^R , and σ_4 is the standard deviation of t_4^R which is assumed known. It then follows that Z^{DIST} is a standardised normal distribution, and *Hosking and Wallis* [1993] suggested using a 90% confidence level for accepting a particular

101 distribution, i.e. if $|Z^{DIST}| \leq 1.64$, a distribution is considered an acceptable candidate
 102 distribution for the region. Although not strictly part of the HW method, the distribution
 103 with the Z^{DIST} score closest to zero is often chosen, but other distributions could be
 104 selected based on other considerations.

105 FIGURE 1 ABOUT HERE

The bias and standard deviation of the regional L-kurtosis value were obtained via Monte Carlo simulations. First a four parameter kappa distribution was specified using the first four L-moment ratios l, τ^R, τ_3^R and τ_4^R . From this kappa distribution a large number, N_{sim} , of homogeneous regions are generated, each representing AMAX data from $i = 1 \dots N$ sites with individual record length n_i . For the m -th simulated region the regional average L skewness, $t_3^{[m]}$, and L kurtosis, $t_4^{[m]}$, are derived, and the bias B_4 and standard deviation σ_4 derived as

$$B_4 = N_{sim}^{-1} \sum_{m=1}^{N_{sim}} (t_4^{[m]} - t_4^R) \quad (9)$$

$$\sigma_4 = \left[(N_{sim} - 1)^{-1} \left\{ \sum_{m=1}^{N_{sim}} (t_4^{[m]} - t_4^R)^2 - N_{sim} B_4^2 \right\} \right]^{1/2} \quad (10)$$

106 *Hosking and Wallis* [1993] used $N_{sim} = 500$, and this was found to be an adequate number
 107 also for this study. The bias correction is likely to be important for short record lengths
 108 and for very skewed data series; see for example Figure 2.7 in *Hosking and Wallis* [1997].

109 *Hosking and Wallis* [1993] emphasised that the assumptions underpinning their GOF
 110 measure are unlikely to be met by real regions, and emphasised therefore that the measure
 111 should not be interpreted as a formal statistical test of goodness of fit. The same qualifier
 112 applies to the new bivariate extension presented in the next section.

3.2. A bivariate extension of the HW measure

The new bivariate extension of the HW measure proposed here is illustrated in the right panel on Figure 1. It is based on the interpretation of a confidence interval as a form of statistical test, and the approximate bivariate normal distribution of L-skewness and L-kurtosis as also utilised by *Liou et al.* [2008]. The confidence region for the bivariate distribution of L-skewness and L-kurtosis is defined by the measure T with a set of bias corrected regional L-moment ratios \mathbf{t}^R against which the theoretical $\boldsymbol{\tau}$ L-moments are compared:

$$T = (\boldsymbol{\tau} - \mathbf{t}^R)^T \boldsymbol{\Omega}^{-1} (\boldsymbol{\tau} - \mathbf{t}^R) \quad (11)$$

113 where $\boldsymbol{\tau}$ is the null hypothesis mean values of L-skewness and L-kurtosis. The components
 114 of the $\boldsymbol{\Omega}$ covariance matrix in Eq.(11) are estimated by means of N_{sim} synthetic samples
 115 generated from a kappa distribution with third and fourth L-moment equal to \mathbf{t}^R . In the
 116 case of perfectly independent observations and homogeneous regions the quantity $(N_{sim} -$
 117 $2)/(2(N_{sim} - 1)) T$ is distributed according to a F -distribution with $(2, N_{sim} - 2)$ degrees
 118 of freedom, i.e. $\frac{N_{sim}-2}{2(N_{sim}-1)} T \sim F_{2, N_{sim}-2}$. For N_{sim} sufficiently large the approximation
 119 $2F_{2, N_{sim}-2} \approx \chi_2^2$ holds, so that the quantity in Eq.(11) can be approximated by a chi-square
 120 distribution: $T \sim \chi_2^2$. The key assumptions behind this approximation are that the region
 121 under study is homogeneous, that a sufficient number of site-years are available and that
 122 a large number of N_{sim} synthetic samples are employed in the procedure to estimate $\boldsymbol{\Omega}$.

123 Utilising the same set of Monte Carlo simulations deployed for calculating the variance
 124 of L-kurtosis in connection with the HW measure, the corresponding bias and variance
 125 of L-skewness, B_3 and σ_3^2 , can be estimated using a similar set of equations as those used

126 for L-kurtosis in Eqs. (9) and (10). The covariance between L-skewness and L-kurtosis
 127 can be estimated as

$$\sigma_{34} = (N_{sim} - 1)^{-1} \left\{ \sum_{m=1}^{N_{sim}} (t_3^{[m]} - t_3^R) (t_4^{[m]} - t_4^R) - N_{sim} B_3 B_4 \right\} \quad (12)$$

For a given significance level α , the $(1 - \alpha)100\%$ confidence ellipse for the bias-corrected regional L-skewness and L-kurtosis, $\mathbf{t}_B^R = (t_3^R - B_3, t_4^R - B_4)$, can be constructed, using the estimated $\mathbf{\Omega}$ covariance matrix and the χ_2^2 approximation discussed above. The $(1 - \alpha)100\%$ confidence ellipse is plotted on the L-moment diagram along with the theoretical relationships between L-skewness and L-kurtosis as used previously in the calculation of the HW measure. If segments of the theoretical line of a specific distribution are located within the circumference of the confidence ellipse then this distribution should be considered as a candidate for the regional distribution. Taking $\boldsymbol{\tau}^{DIST} = (\tau_3, \tau_4^{DIST}(\tau_3))$ to be the vector of possible (τ_3, τ_4) values for a distribution, if the minimum value of the Mahalanobis distance

$$D^{DIST} = (\boldsymbol{\tau}^{DIST} - \mathbf{t}_B^R)^T \mathbf{\Omega}^{-1} (\boldsymbol{\tau}^{DIST} - \mathbf{t}_B^R) \quad (13)$$

128 is smaller than the critical $\chi_{2,1-\alpha}^2$ quantile, the distribution *DIST* can be considered to be
 129 a possible candidate distribution at a significance level α . The final choice of distribution
 130 is determined by selecting from among all the theoretical curves, $(\tau_3, \tau_4^{DIST}(\tau_3))$ which lie
 131 within the $(1 - \alpha)100\%$ ellipsoid, the point with the shortest D^{DIST} value. As with the
 132 HW measure, other accepted distributions could be chosen if there were any particular
 133 reason to do so.

134 The concept is also illustrated on Figure 2 where the right panel shows the difference
135 between the regional L-moment ratios and the theoretical lines representing various 3-
136 parameter distributions. In Figure 2 the minimum distance is obtained for the GEV
137 distribution, which is chosen as the regional distribution accordingly.

138 FIGURE 2 ABOUT HERE

139 Only distributions with theoretical lines located within the $(1 - \alpha)100\%$ confidence
140 region can be chosen as candidate distributions. Thus, in some cases the new bivariate
141 measure may fail to accept any of the considered distributions as suitable for a particular
142 region for the given confidence level.

4. Comparison of GOF measures

143 The performance of the new bivariate measure was evaluated and compared to the
144 original HW measure using a set of Monte Carlo simulations and a significance level of
145 $\alpha = 10\%$. Firstly, three different homogeneous regions were defined to mimic the regions
146 used by *Hosking and Wallis* [1993] in their evaluation of the HW measure. Each region
147 consists of $N = 21$ sites and each site has a record length of $n = 30$ years. Each of
148 the three region is defined by a specified set of regional values for L CV and L-skewness
149 ($(\tau = 0.10, \tau_3 = 0.05)$, $(\tau = 0.20, \tau_3 = 0.20)$ and $(\tau = 0.30, \tau_3 = 0.30)$), and one of four
150 different parent distributions: Generalised Logistic (GLO), Generalised Extreme Value
151 (GEV), Generalised Normal (GNO) or a Pearson Type III (PE3) distribution. The twelve
152 resulting regions are listed in the first four columns in Tables 1 and 2. For each region,
153 Monte Carlo simulations are used to generate 1000 replicas of the region from the specified
154 parent distribution. For each one of the 1000 replica regions, both the original HW
155 measure and the new bivariate measure were evaluated. Both the number of times a

156 particular distribution was accepted as a parent distribution and the number of times
157 each distribution was chosen as the best fitting distribution were recorded. The results
158 are shown in Table 1 (original HW measure), and Table 2 (new bivariate measure).

159 TABLE 1 ABOUT HERE

160 TABLE 2 ABOUT HERE

161 The results obtained for the original HW measure in Table 1 are very similar to the
162 results presented by *Hosking and Wallis* [1997], but differ in one aspect. By design the
163 new bivariate version cannot choose a particular distribution without first accepting it as
164 a possible candidate. However, this distinction was not enforced by *Hosking and Wallis*
165 [1993] who reported that in some cases the GLO distribution had been chosen more times
166 than it had been accepted. Thus, to enable a direct comparison of the two measures
167 in this study, the original HW measure was only allowed to choose a distribution if this
168 distribution had first been accepted by the same measure as a possible candidate.

169 For eleven of the twelve considered regions the new bivariate measure performs better
170 than the original HW measure, meaning that the correct regional distribution is cho-
171 sen more often by the new measure. While the differences are consistent they are not
172 necessarily large, varying from 1% to 14%.

173 Given that no additional simulation effort is required when evaluating the GOF using
174 the new measure compared to the original HW measure, the results shown in Table 1 and
175 2 suggest that the new bivariate measure should be used in preference to the original HW
176 measure. However, it is necessary to discuss possible situations where the original HW
177 measure appears to outperform the new bivariate measure.

178 Similarly to *Hosking and Wallis* [1993], the new bivariate version was found to accept the
179 GLO distribution less frequent than other parent distributions. *Hosking and Wallis* [1993]
180 suggested that this might be caused by underestimation of σ_4 , but did not investigate
181 further. An alternative explanation might relate to the asymmetric influence of the bias
182 correction on the L-moment ratios. Figure 2.7 in *Hosking and Wallis* [1997] shows that the
183 effect of the bias is more pronounced for higher value of L-skewness and L-kurtosis. As the
184 GLO distribution is characterised by higher L-kurtosis values than the other 3 parameter
185 distributions (the theoretical GLO lines is located above the other 3 parameter distribution
186 lines in the L-moment diagram), sample values generated from a GLO distribution are
187 therefore more likely to be moved even further up on the L-moment diagram as a result
188 of the bias correction. Figure 3 shows the regional average L-skewness and L-kurtosis for
189 five Monte Carlo generated regions from each of the three regions defined in Table 1. The
190 plot on the left side shows the result when the AMAX events are generated from a GEV
191 distribution, and the right side shows the results when generating AMAX events from a
192 GLO distribution. The points represent the bias corrected values, and the arrows point
193 to the location of the initial uncorrected sample values.

194 FIGURE 3 HERE

195 From the Figures it can be seen that samples generated from the GLO distribution are
196 located higher on the L-moment diagram, and therefore are subject to a larger degree
197 of bias correction. In some instances the bias correction is so large that the ellipse cor-
198 responding to the 90% confidence region (not shown) is moved so far that it no longer
199 bisects the GLO line, suggesting that the GLO distribution is no longer considered suit-
200 able. This might be the reason why the GLO distribution is chosen less frequently than

201 the other distributions, but it does not explain why the performance of the new bivariate
202 measure is not as good as the original HW measure for the third region, consisting of a
203 very skewed GLO distribution ($\tau_3 = 0.30$).

5. Assessing the effect of intersite correlation

204 The importance of intersite correlation between AMAX series from different sites within
205 a region has been discussed by several authors, e.g *Stedinger* [1983], *Hosking and Wallis*
206 [1988], *Kjeldsen and Jones* [2006], *Castellarin et al.* [2008]. From these studies it is well-
207 understood that the effect of intersite correlation is primarily to increase the variance of
208 the regional L-moment ratios. For the goodness-of-fit measures discussed in this study,
209 the effect of increased variance of L-moment ratios should lead to a decrease in the ability
210 of these measures to discriminate between distribution types.

211 A set of Monte Carlo simulations was used to investigate the effect of intersite correlation
212 on the power of the original and new bivariate measure. The algorithm used for generating
213 cross-correlated AMAX events from the N sites within a homogeneous region was adopted
214 from *Hosking and Wallis* [1997], and also used by *Castellarin et al.* [2008] in a study of
215 effects of intersite correlation on the performance of a measure for homogeneity. Repeated
216 Monte Carlo simulations were conducted assuming an average cross correlation between
217 0.0 to 0.80 with a step-length of 0.10 (i.e. nine repetitions) using the same three regions as
218 for the independent case discussed above, i.e. $(\tau = 0.10, \tau_3 = 0.05)$, $(\tau = 0.20, \tau_3 = 0.20)$
219 and $(\tau = 0.30, \tau_3 = 0.30)$ assuming one of the four distributions: GLO, GEV, GNO or
220 PE3. This experimental setup results in a total of 108 different regions. For each region,
221 1000 replica regions were generated, then the two GOF measures were evaluated, and the
222 rate of choosing the correct regional distribution recorded. Figure 4 shows the percentage

223 of the 1000 regions where the correct distribution type was selected by each of the two
224 measures.

225 FIGURE 4 ABOUT HERE

226 For all four distributions (GLO, GEV, GNO and PE3) both measures are reasonably
227 robust to the existence of intersite correlation when this is below about 0.40. For higher
228 degrees of correlation the success rate of both measures starts to decline.

229 In general the new bivariate measure proposed in this study performs better than the
230 original HW measure, except for the case of the GLO distribution for the region with
231 high L-CV and L-skewness population parameters as already discussed. The performance
232 of the two measures declines at a similar rate for higher intersite correlations: so for all
233 levels of intersite variation the new bivariate measure is preferable.

6. Case studies

6.1. Example 1: Regional distribution of flood flow data in Central Italy

234 The new bivariate measure is applied to AMAX peak flow series from 22 flow gauging
235 stations located in a Central part of Italy. These stations correspond to the catchments
236 of region E described in *Castellarin* [2007], and have a record length between 15 and 74
237 years, with an average record length of 33.5 years. The original HW and the new bivariate
238 measures are both applied to these series. Figure 5 shows the L-moments diagram with the
239 ellipse corresponding to the 90% confidence region obtained from the bivariate measure.

240 FIGURE 5 ABOUT HERE

241 TABLE 3 ABOUT HERE

242 The results in Figure 5 and Table 3 show that for this dataset, both the GEV and
243 the GNO distributions could be accepted as the regional distributions, but the the GEV
244 distribution is the more likely candidate.

6.2. Example 2: A national distribution of UK flood data

245 The new new bivariate measure was applied on annual maximum (AMAX) series of
246 peak flow from 564 rural catchments located through-out the UK. For each catchment,
247 a site specific hydrological region (e.g. a pooling group) was formed based on hydro-
248 logical similarity using the similarity measure developed by *Kjeldsen and Jones* [2009]
249 and calculated using four different catchment descriptors: the catchment area (km²), the
250 standard annual average rainfall as measured between 1961 and 1990 (mm), an index of
251 flood attenuation from upstream lakes and reservoirs, and the areal extent of floodplains
252 in the upstream catchment defined by the 100-year flood level adopted from an existing
253 national floodplain map.

254 A pooling group for each of the 564 catchments is formed by adding catchments from
255 the entire database, starting with the most similar and continuing to add catchments
256 until the total sum of AMAX events included in the pooling group exceeds 500. With
257 an average record length of 36 years, a pooling group typically consists of between 12-15
258 catchments.

259 A first visual assessment of candidate distributions can be obtained by plotting the pairs
260 of average L-skewness and L-kurtosis for each of the 564 pooling groups on a L-moment
261 diagram as shown in Figure 6. From the L-moment diagram it is evident that the regional
262 L-moment ratios generally plot between the two lines representing the GLO and the GEV
263 distributions, both of which have previously been adopted as standard distributions for

264 regional and pooled flood frequency estimation in the UK [*Natural Environment Research*
265 *Council, 1975; Institute of Hydrology, 1999*]. Generally, the average correlation between
266 the overlapping AMAX series within each pooling group is below 0.4 suggesting, with
267 reference to the results in Figure 4, that the performance of the new GOF measure should
268 not be unduly influenced by cross-correlation.

269 FIGURE 6 ABOUT HERE

270 A more quantitative assessment of the distribution type was undertaken by comparing
271 the rate of accepting and choosing different distribution types using both the original
272 HW measure and the new bivariate extension presented in this study. Applying the two
273 measures to each of the 564 pooling groups, the percentage of pooling groups where a
274 particular distribution is accepted and chosen is shown in Table 4.

275 TABLE 4 ABOUT HERE

276 The results in Table 4 show that both measures select the GLO distribution most
277 frequently as the most suitable regional distribution. For the GNO and PE3 distributions,
278 the selection rates are very similar for the two measures, and in any case much lower than
279 for the GLO and GEV distributions. The new bivariate measure shows that the GLO and
280 GEV distributions are accepted as candidate distributions an almost identical number of
281 times, but that the GLO distribution is the preferred distribution as it is chosen more
282 often than the GEV distribution. For 28 out of the 564 catchments ($\approx 5\%$), the new
283 bivariate measure found that none of the four distributions adequately fitted the data.
284 The original HW measure selects the GLO more often than the new bivariate measure, and
285 thus gives more support to the GLO distribution as the default choice in UK catchments;
286 for example if conducting a regional analysis in an ungauged catchment. The results

287 shown in Table 4 combined with a visual inspection of the scatter of pooled L-moment
288 ratios in Figure 6 suggests that the GLO distribution might not always be the best choice
289 for UK catchments, and that the GEV distribution could also be considered in most cases.

7. Conclusion

290 This paper presented a new GOF measure for regional frequency distributions based
291 on L-moment ratios and with a direct graphical interpretation using the L-moment ratio
292 diagram. Based on a series of Monte Carlo simulations from homogeneous regions the
293 new measure was found to provide a modest, but consistent, improvement in the ability
294 to detect the underlying regional distribution when compared to the performance of the
295 original one-dimensional GOF measure presented by *Hosking and Wallis* [1993]. This
296 additional power was obtained utilising exactly the same set of Monte Carlo simulations
297 as the original HW measure. Additional Monte Carlo simulations from regions where
298 AMAX events are correlated across sites demonstrated that the performance of the new
299 measure is sustained for regions with a level of correlation akin to that found in most UK
300 pooling groups. As these pooling groups are made up of data from a relatively confined
301 geographical region, it is expected that similar or less correlation is found in many other
302 real world regions.

303 Further research should investigate the relatively poor performance of the new measure
304 for detecting the GLO distribution in regions characterised by high values of L-skewness.
305 Another important topic to investigate is if the more generalised set of weights in Eq. (6)
306 can be developed to improve performance in cross-correlated and heterogeneous regions.

307 **Acknowledgments.** The authors would like to thank Attilio Castellarin (at-
308 tilio.castellarin@unibo.it) and the UK measuring authority's HiFlows-UK database
309 (http://www.ceh.ac.uk/data/nrfa/peakflow_overview.html) for providing access to the
310 Italian and UK flood flow data, respectively. Three anonymous reviewers are acknowl-
311 edged for helpful criticism of an earlier version of the manuscript.

References

- 312 Castellarin, A. (2007), Probabilistic envelope curves for design flood estimation at un-
313 gauged sites, *Water Resources Research*, *43*(4), 1944–7973.
- 314 Castellarin, A., D. Burn, and A. Brath (2008), Homogeneity testing: How homogeneous
315 do heterogeneous cross-correlated regions seem?, *Journal of Hydrology*, *360*(1), 67–76.
- 316 Hosking, J. R. (1990), L-moments: analysis and estimation of distributions using lin-
317 ear combinations of order statistics, *Journal of the Royal Statistical Society. Series B*
318 (*Methodological*), pp. 105–124.
- 319 Hosking, J. (1986), The theory of probability weighted moments, *IBM Res. Rep. RC12210*,
320 *IBM, Yorktown Heights, NY*.
- 321 Hosking, J. R. M., and J. R. Wallis (1997), *Regional frequency analysis: an approach based*
322 *on L-moments*, Cambridge University Press.
- 323 Hosking, J., and J. Wallis (1993), Some statistics useful in regional frequency analysis,
324 *Water Resources Research*, *29*(2), 271–281.
- 325 Hosking, J., and J. Wallis (1988), The effect of intersite dependence on regional flood
326 frequency analysis, *Water Resources Research*, *24*(4), 588–600.
- 327 Institute of Hydrology (1999), *Flood Estimation Handbook*, Institute of Hydrology.

- 328 Kjeldsen, T. R., and D. A. Jones (2006), Prediction uncertainty in a median-based index
329 flood method using L moments, *Water resources research*, 42(7). W07414.
- 330 Kjeldsen, T. R., and D. A. Jones (2009), A formal statistical model for pooled analysis of
331 extreme floods, *Hydrology Research*, 40(5), 465–480.
- 332 Kumar, R., C. Chatterjee, S. Kumar, A. Lohani, and R. Singh (2003), Development
333 of regional flood frequency relationships using L-moments for Middle Ganga Plains
334 Subzone 1 (f) of India, *Water Resources Management*, 17(4), 243–257.
- 335 Liou, J.-J., Y.-C. Wu, and K.-S. Cheng (2008), Establishing acceptance regions for L-
336 moments based goodness-of-fit tests by stochastic simulation, *Journal of Hydrology*,
337 355(1), 49–62.
- 338 Madsen, H., C. P. Pearson, and D. Rosbjerg (1997), Comparison of annual maximum
339 series and partial duration series methods for modeling extreme hydrological events 2.
340 Regional modeling, *Water Resources Research*, 33(4), 759–769.
- 341 Mkhandi, S., R. Kachroo, and T. Gunasekara (2000), Flood frequency analysis of southern
342 Africa: II. identification of regional distributions, *Hydrological sciences journal*, 45(3),
343 449–464.
- 344 Natural Environment Research Council (1975), *Flood Studies Report, (5 Volumes)*, Nat-
345 ural Environment Research Council, London, UK.
- 346 Peel, M. C., Q. Wang, R. M. Vogel, and T. A. McMahon (2001), The utility of L-moment
347 ratio diagrams for selecting a regional probability distribution, *Hydrological sciences*
348 *journal*, 46(1), 147–155.
- 349 Sankarasubramanian, A., and K. Srinivasan (1999), Investigation and comparison of sam-
350 pling properties of L-moments and conventional moments, *Journal of Hydrology*, 218(1),

351 13–34.

352 Stedinger, J. R. (1983), Estimating a regional flood frequency distribution, *Water Re-*
353 *sources Research*, 19(2), 503–510.

354 Vogel, R. M., and N. M. Fennessey (1993), L moment diagrams should replace product
355 moment diagrams, *Water Resources Research*, 29(6), 1745–1752.

356 Vogel, R. M., W. O. Thomas Jr, and T. A. McMahon (1993), Flood-flow frequency model
357 selection in Southwestern United states, *Journal of Water Resources Planning and Man-*
358 *agement*, 119(3), 353–366.

359 Wang, D., and A. D. Hutson (2013), Joint confidence region estimation of L-moment
360 ratios with an extension to right censored data, *Journal of Applied Statistics*, 40(2),
361 368–379.

362 Wu, Y.-C., J.-J. Liou, Y.-F. Su, and K.-S. Cheng (2012), Establishing acceptance re-
363 gions for L-moments based goodness-of-fit tests for the Pearson type III distribution,
364 *Stochastic Environmental Research and Risk Assessment*, 26(6), 873–885.

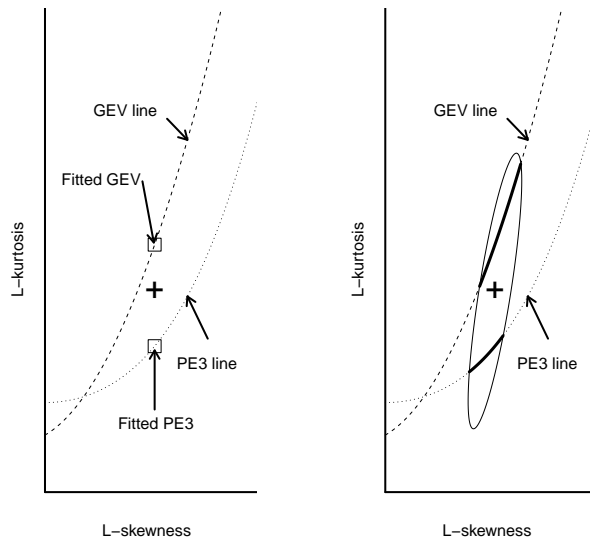


Figure 1. Explanatory sketches for HW GOF measure (left), adopted from *Hosking and Wallis* [1993], and (right) the new bivariate GOF measure. In the right panel, the bold line segments located with the circumsphere of the ellipsoid are within the 90% confidence region of the regional L-moment ratios, and thus potentially accepted as regional distributions. In both figures the bold cross represents the average sample values of L-skewness and L-kurtosis.

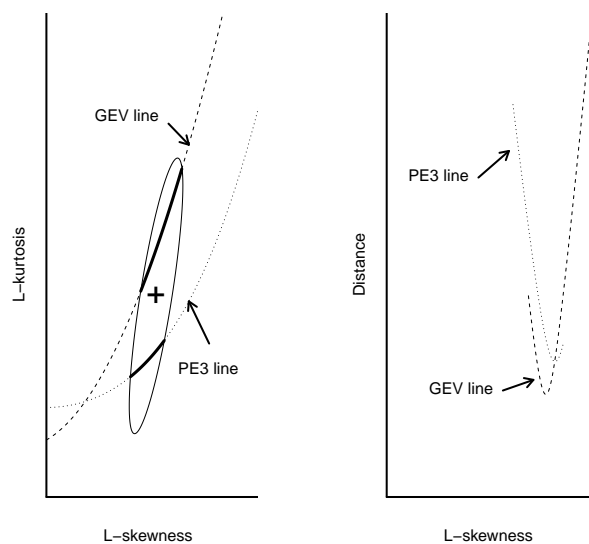


Figure 2. Accepted candidate distributions are identified where segments of the theoretical distribution lines are located within the confidence region, shown as bold line-segments on the left figure. The final choice of distribution is based on the minimum distance between regional L-moment ratios and the theoretical distribution within the region of acceptance as shown on the right figure.

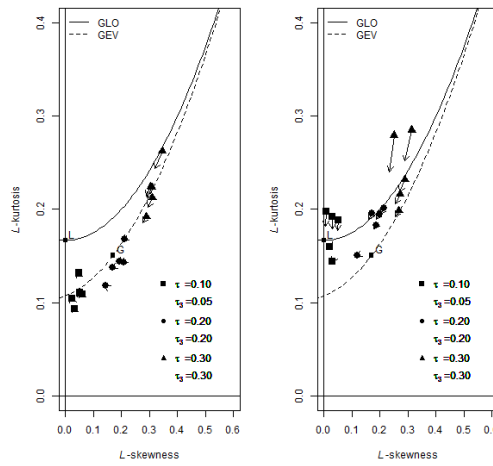


Figure 3. Regional estimates of L-skewness and L-kurtosis using AMAX data generated from a GEV distribution (left) and a GLO distribution (right) for three different homogeneous regions. The points represent the bias correct values of t_3^R and t_4^R and the arrows point to the initial uncorrected sample values.

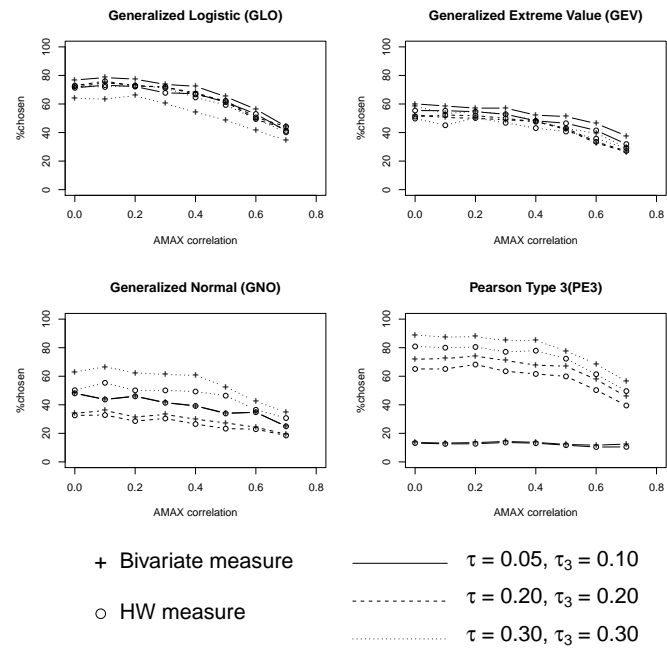


Figure 4. Comparison of the performance of the original HW and the new bivariate GOF measures in three different regions shown as a function of intersite correlation between AMAX series within each region.

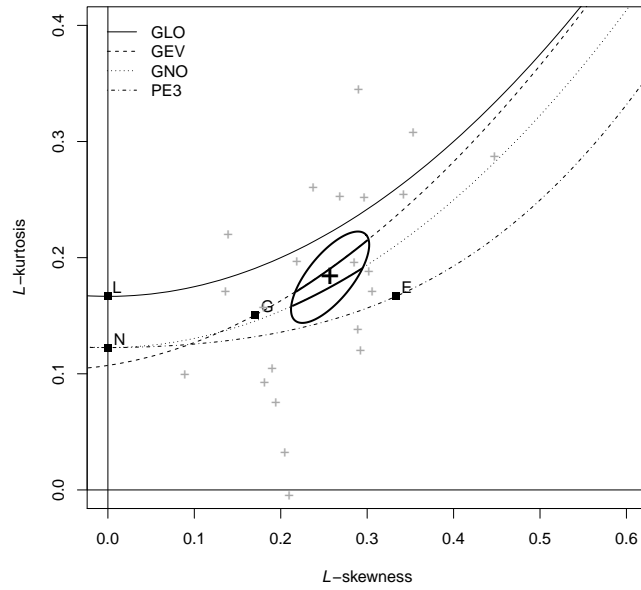


Figure 5. L-moment diagram showing L-moment ratios for the 22 Italian catchments and the corresponding 90% confidence region. The thick line segments represent the segments of the theoretical distributions that fall within the 90% confidence region.

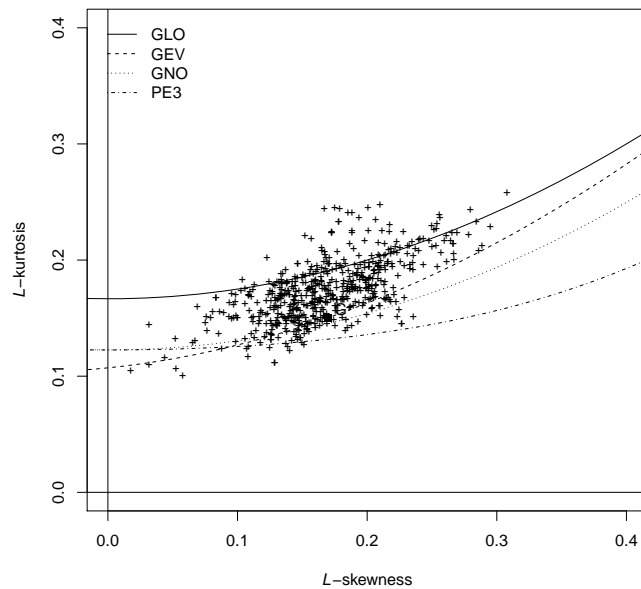


Figure 6. Regional L-moment ratios for each of the 564 UK pooling groups plotted on a L-moment diagram.

Table 1. Simulation results for the original HW GOF measure showing percentage of simulations where a particular distribution is accepted and chosen.

τ	τ_3		% Accepted				% Chosen			
			GLO	GEV	GNO	PE3	GLO	GEV	GNO	PE3
0.1	0.05	GLO	75	3	12	10	73	0	9	0
		GEV	2	87	79	81	2	52	24	14
		GNO	9	81	88	88	7	35	45	13
		PE3	7	83	88	88	6	35	41	16
0.2	0.2	GLO	78	26	15	4	72	12	1	0
		GEV	34	93	86	51	17	51	19	13
		GNO	15	90	92	73	5	35	33	27
		PE3	1	52	72	89	0	8	21	65
0.3	0.3	GLO	84	54	17	1	73	13	1	0
		GEV	74	94	67	10	38	47	14	1
		GNO	31	88	95	34	5	33	54	9
		PE3	0	6	38	93	0	0	14	81

Table 2. Simulation results for the new bivariate GOF measure showing percentage of simulations where a particular distribution is accepted and chosen.

τ	τ_3		% Accepted				% Chosen			
			GLO	GEV	GNO	PE3	GLO	GEV	GNO	PE3
0.1	0.05	GLO	85	9	25	22	79	0	9	0
		GEV	5	96	88	90	1	56	24	15
		GNO	18	92	96	96	6	34	45	14
		PE3	13	94	95	95	6	36	41	16
0.2	0.2	GLO	82	38	24	8	73	14	1	0
		GEV	31	95	93	67	11	50	23	16
		GNO	12	90	96	84	3	30	37	30
		PE3	0	50	75	95	0	5	20	72
0.3	0.3	GLO	84	65	24	2	64	24	2	0
		GEV	54	94	75	15	20	54	25	2
		GNO	11	66	96	47	1	21	64	14
		PE3	0	1	23	95	0	0	8	87

Table 3. Comparison of the original HW and the new bivariate GOF measures on a homogeneous region consisting of 22 Italian catchments. Numbers indicate values of the GOF measures and bold fonts highlight the chosen distributions.

	GLO	GEV	GNO	PE3
Original HW	1.86	0.10	-0.69	-2.14
New Bivariate	-	0.32	0.39	-

Table 4. Comparison of the new bivariate GOF measure and the original HW measure. Numbers represent percentages of the 564 pooling groups accepted and chosen by the new measure. Numbers in () refer to the corresponding results obtained using the original HW measure.

	GLO	GEV	GNO	PE3
Accepted	74(70)	79(67)	71(58)	50(36)
Chosen	49(53)	31(27)	12(11)	4(4)